Available online at www.sciencedirect.com
SCIENCE DIRECT®
Mathematical and Computer Modelling 42 (2005) 1359–1374
MATHEMATICAL AND COMPUTER MODELLING
www.elsevier.com/locate/mcm

Dynamical Analysis and Impulsive Control of a New Hyperchaotic System

YUXIA LI
Department of Automation
Binzhou University
Binzhou, Shandong 256600, P.R. China
and
College of Information and Electrical Engineering
Shandong University of Science and Technology
Qingdao, Shandong 266510, P.R. China

XINZHI LIU*
Department of Applied Mathematics
University of Waterloo
Waterloo, Ontario, Canada N2L 3G1
xzliu@uwaterloo.ca

HONGTAO ZHANG
Department of Control Science and Engineering
Huazhong University of Science and Technology
Wuhan, Hubei 430074, P.R. China

(Received August 2004; accepted September 2004)

Abstract—A new hyperchaotic system has been proposed recently. It is generated by controlling a unified chaotic system to hyperchaotic via a simple technique using a sinusoidal parameter perturbation control input. In this paper, we further investigate its dynamical behaviors, its circuit implementation and its impulsive control. Different chaotic attractors are illustrated by both numerical simulations and electronic experiments. It is also shown that the new hyperchaotic system can be stabilized by impulsive control.

Keywords—Hyperchaotic system, Chaotic attractor, Impulsive control.

1. INTRODUCTION

Hyperchaotic system is usually classified as a chaotic system with more than one positive Lyapunov exponent, indicating that the chaotic dynamics of the system are expanded in more than one direction giving rise to a more complex attractor. Hyperchaotic Chua's circuit [1,2] and Rossler system [3] are two well known examples of hyperchaotic models.

*Author to whom all correspondence should be addressed.
Research supported by NSERC-Canada.

0895-7177/05/$ - see front matter Typeset by AMS-TEX
doi:10.1016/j.mcm.2004.09.011

Chaos and hyperchaos have been studied with increasing interest in recent years, in the fields of nonlinear circuits [4], secure communications [5,6], lasers [7], Colpitts oscillators [8], control [9,10], and synchronization [11,12]. Due to its great potential in applications, the generation of hyperchaos in circuits has become a focused topic for research [1,2,4,13,14]. Creating a hyperchaotic attractor, in particular, purposefully design a hyperchaotic system based on an originally chaotic but nonhyperchaotic system by a simple means, is a theoretically very attractive and yet technically quite challenging problem.

Quite recently, a new hyperchaotic system is presented in [13], which is generated by controlling a unified chaotic system to hyperchaotic via a simple technique using a sinusoidal parameter perturbation control input. The original chaotic system is a three-dimensional autonomous system that has a broad spectrum of chaotic behaviors with the Lorenz and the Chen systems as two extremes of the spectrum [15]. The control input is a simple sinusoidal function $\cos(\omega t)$ with a constant parameter ω. In this paper, we further investigate its dynamical behaviors, its circuit implementation and its impulsive control. The organization of the paper is as follows. In Section 2, we discuss the special features of the new hyperchaotic system and its circuit implementation. Different chaotic attractors are illustrated by both numerical simulations and electronic experiments. Then we explore, in Section 3, some of the basic dynamical properties of the system. Impulsive control is considered in Section 4, where it is shown that the new hyperchaotic system can be stabilized by impulsive control.

2. THE HYPERCHAOTIC UNIFIED SYSTEM

2.1. Some Special Features of the New Hyperchaotic System

The hyperchaotic unified system was presented in [13], which is described as follows,

$$\begin{aligned} \dot{x} &= (25 - 10\cos(\omega t))(y - x), \\ \dot{y} &= (17.5\cos(\omega t) + 10.5)x \\ &\quad - xz + (13.3 - 14\cos(\omega t))y, \\ \dot{z} &= xy - \frac{8}{3}z, \end{aligned} \tag{1}$$

where the control function $a = \cos(\omega t) \in [-1, 1]$. This system can be generalized in the following form,

$$\begin{bmatrix} \dot{x} \\ \dot{y} \\ \dot{z} \end{bmatrix} = \begin{bmatrix} a_{11} & a_{12} & 0 \\ a_{21} & a_{22} & 0 \\ 0 & 0 & a_{33} \end{bmatrix} \begin{bmatrix} x \\ y \\ z \end{bmatrix} + x \begin{bmatrix} 0 & 0 & 0 \\ 0 & 0 & -1 \\ 0 & 1 & 0 \end{bmatrix} \begin{bmatrix} x \\ y \\ z \end{bmatrix}, \tag{2}$$

where $a_{11} = -(25 - 10a)$, $a_{12} = (25 - 10a)$, $a_{21} = (17.5a + 10.5)$, $a_{22} = (13.3 - 14a)$, and $a_{33} = -8/3$.

System (1) has the following special features.

(i) The system presents a simple technique using a sinusoidal parameter perturbation control input to drive a unified chaotic system to hyperchaotic.

(ii) The original chaotic system is a three-dimensional autonomous system that has a broad spectrum of chaotic behaviors with the Lorenz and the Chen systems as two extremes of the spectrum.

(iii) The control input is a simple sinusoidal function $\cos(\omega t)$ with a constant parameter ω.

(iv) The system is a hyperchaotic system when $\omega \in [0.55, 6.33]$. With $\omega = 3$, the hyperchaotic attractors are shown in Figure 1.

(v) From the bifurcation analysis of the system [13,16], we observed that the transition from chaos to hyperchaos is soft and continuous.

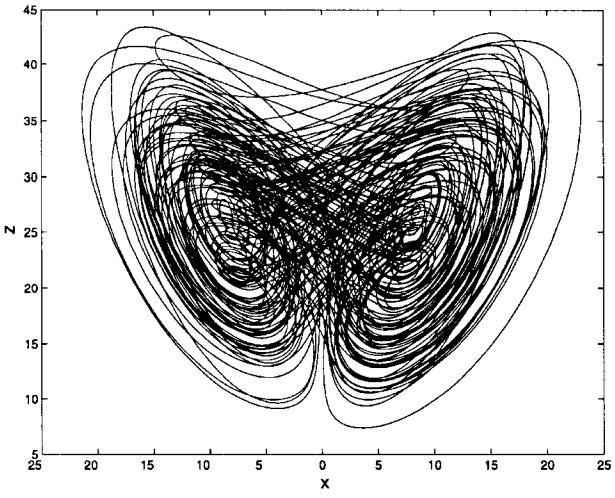

(a) $x - z$ plane.

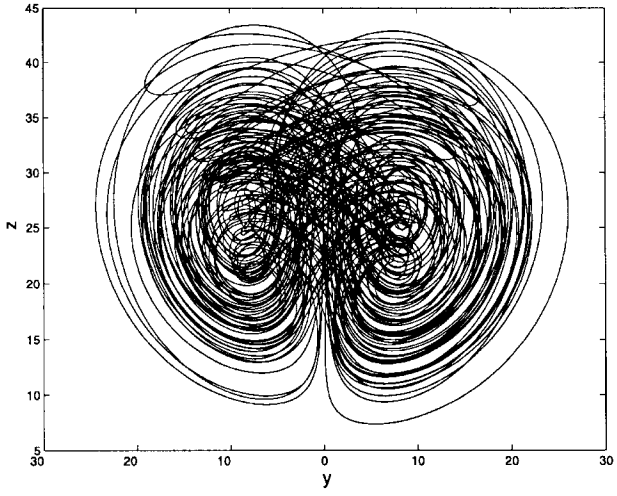

(b) $y - z$ plane.

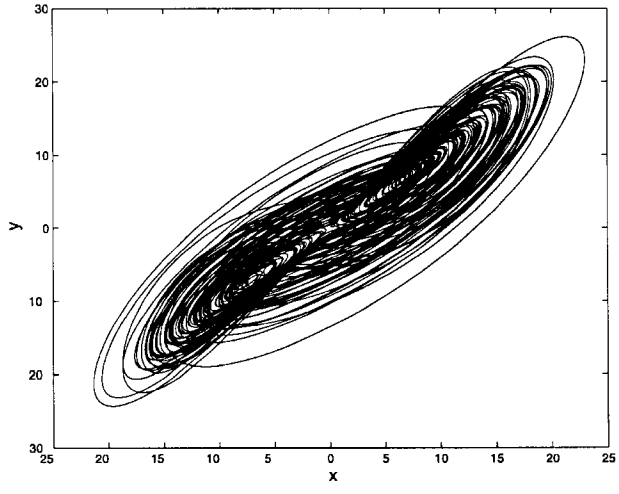

(c) $x - y$ plane.

Figure 1. Phase portraits of the hyperchaotic system (1) with $\omega = 3$.

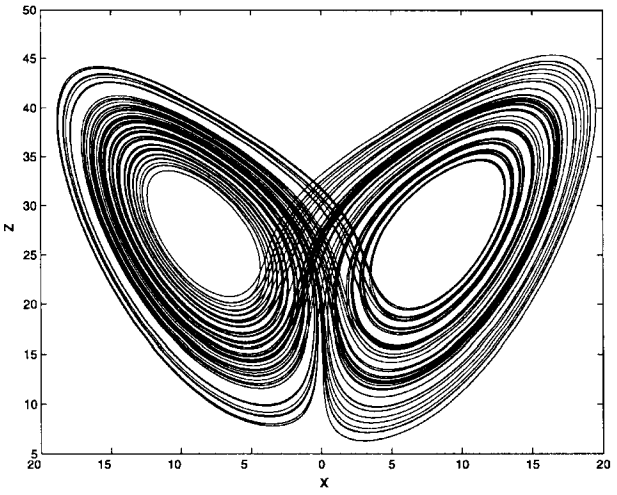

(a) $b = 8/3$, a=1.

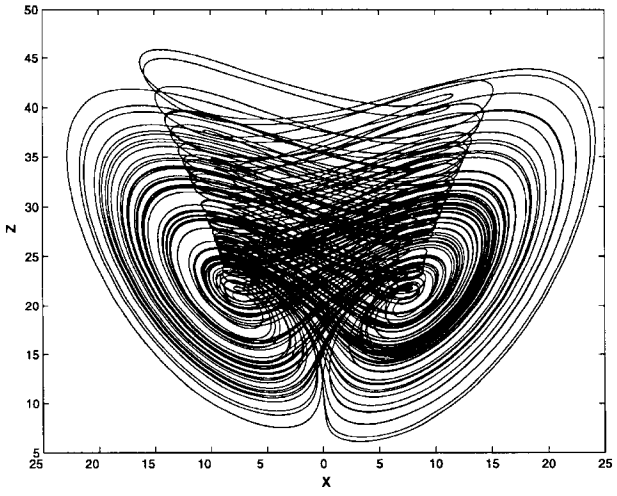

(b) $b = 8/3, a = 1$.

Figure 2. Phase portraits of system (1).

(vi) According to the criterion of Vanček and Čelikovský [17], when

$$t \in \left[\frac{1}{\omega}\left(2n\pi - \frac{\pi}{2}\right)\left(\frac{1}{\omega}\right)\left(2n\pi + \frac{\pi}{2}\right)\right],$$

and n is an integer, system (1) is a generalized Lorenz system, with an attractor as shown in Figure 2a, when $t \in [(1/\omega)(2n\pi + \pi/2), (1/\omega)(2n\pi + 3\pi/2)]$ and n is an integer, system (1) is a generalized Chen system, with an attractor as shown in Figure 2b.

2.2. Circuit Implementation of System (1)

The hyperchaotic system (1), has also been confirmed by electronic circuit experiment [13], as shown in Figure 3. The occurrence of the hyperchaotic attractor can be obtained, as shown in Figures 4a–4h. The operational amplifiers perform the operations of addition, subtraction, and integration. The nonlinear terms in the equation are implemented mainly with the analog multipliers.

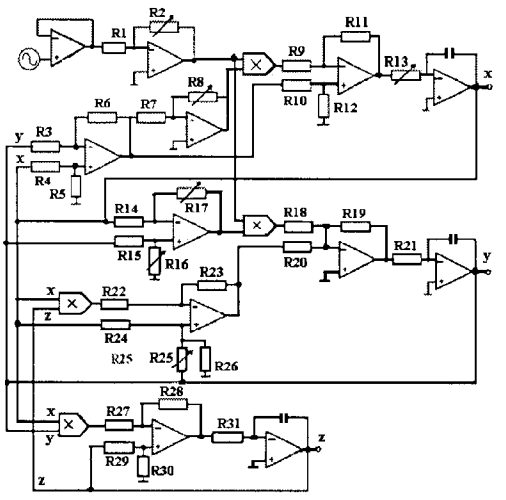

Figure 3. Circuitry realization of the unified hyperchaotic system (3). Resisters ($k\Omega$): $R3$, $R4$, $R5$, $R6$, $R9$, $R10$, $R11$, $R12$, $R18$, $R19$, $R20$, $R21$, $R23$, $R28$, $R29$, $R31 = 10$, $R1 = 2$, $R2 = 6.99$, $R7$, $R14$, $R15$, $R22$, $R27 = 1$, $R8 = 14.29$, $R13 = 3.80$, $R16 = 36.3$, $R17 = 59.2$, $R24 = 3.3$, $R25 = 1.487$, $R26 = 0.172$, $R30 = 0.288$; Capacitors (nF): C_1, C_2, $C_3 = 1$. Op-Amps (1) (12): TL084; Multipliers: AD633.

3. BASIC DYNAMICAL BEHAVIORS OF THE HYPERCHAOTIC UNIFIED SYSTEM

3.1. Symmetry and Invariance

First, note the invariance of the system under the transformation $(x, y, z) \mapsto (-x, -y, z)$, i.e., under reflection in the z-axis. The symmetry persists for all values of the system parameters. Also, it is clear that the z-axis itself is an orbit, i.e., if $x = y = 0$ at $t = 0$, then $x = y = 0$, for all $t > 0$. Moreover, the orbit on the z-axis tends to the origin as $t \to \infty$.

3.2. Dissipativity and the Existence of Attractor

We notice that

$$\nabla V = \frac{\partial \dot{x}}{\partial x} + \frac{\partial \dot{y}}{\partial y} + \frac{\partial \dot{z}}{\partial z} = -\frac{43.1 + 4\cos(\omega t)}{3} < 0.$$

So, with $a = \cos(\omega t) \in [-1, 1]$, system (1) is dissipative, with an exponential contraction rate,

$$\frac{dV}{dt} = -\left(\frac{43.1 + 4a}{3}\right) V.$$

That is, a volume element V_0 is contracted by the flow into a volume element $V_0 e^{-(43.1+4a/3)t}$ in time t. This means that each volume containing the system trajectory shrinks to zero as $t \to \infty$ at an exponential rate $-(43.1 + 4a/3)$. Therefore, all system orbits are ultimately confined to a specific subset having zero volume and the asymptotic motion settles onto an attractor.

3.3. Equilibria and Stability

The equilibria of system (1) can be obtained by making the vector field of (1) zero, which leads to

$$\begin{aligned} (25 - 10\cos(\omega t))(y - x) &= 0, \\ (17.5\cos(\omega t) + 10.5)x - xz + (13.3 - 14\cos(\omega t))y &= 0, \\ xy - 8/3z &= 0. \end{aligned}$$

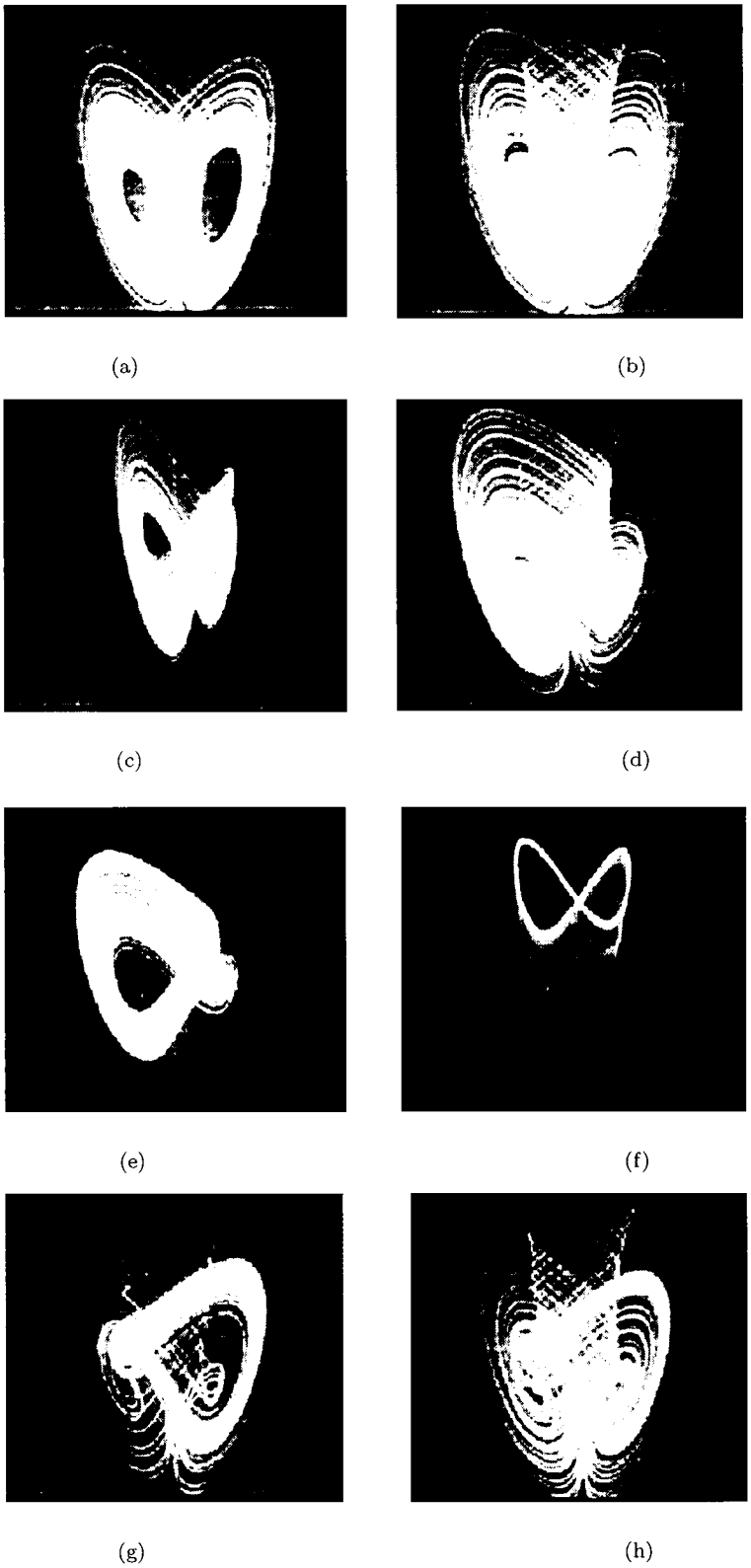

Phase portraits of the unified chaotic system (1) measured with the experimental setup in the $x - z$ plane: (a) Lorenz-like attractor; (b) Chen-like attractor: (c) Lü-like attractor; (d)–(h): transition process. The scales of both vertical and horizontal axes are 0.2 V/div. The supplies of all active devices are ± 14 volts. The frequency of controlling signal is 0.5 Hz.

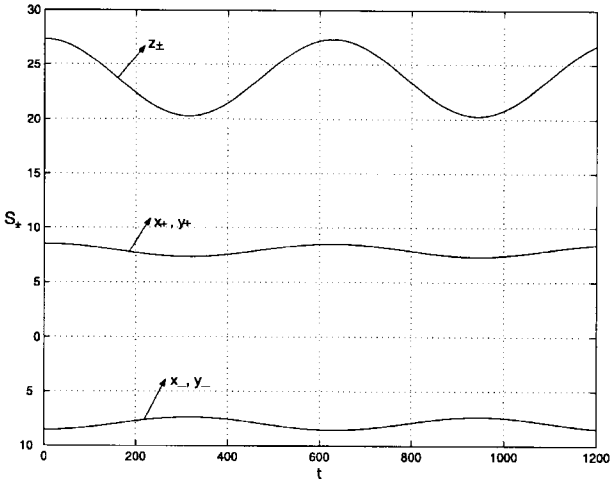

Figure 5. The equilibria $S_{\pm}$ of system (1).

Obviously, system (1) has three equilibria,

$$
\begin{aligned}
&S_0\,(0,0,0)\,,\\
&S_-\left(-\sqrt{\frac{8}{3}\,(23.8+3.5\cos(\omega t))},\right.\\
&\left.q-\sqrt{\frac{8}{3}\,(23.8+3.5\cos(\omega t))},(23.8+3.5\cos(\omega t))\right),\\
&S_+\left(\sqrt{\frac{8}{3}\,(23.8+3.5\cos(\omega t))},\right.\\
&\left.\sqrt{\frac{8}{3}\,(23.8+3.5\cos(\omega t))},(23.8+3.5\cos(\omega t))\right).
\end{aligned}
$$

In which two equilibria, S_- and S_+, are symmetrically placed with respect to the z-axis, as shown in Figure 5.

Let us now study their stability, i.e., the nature of the eigenspaces presented in the neighborhood of each equilibrium point. The Jacobian matrix for system (1) can be written as

$$
J=\begin{bmatrix}
-(25-10\cos(\omega t)) & (25-10\cos(\omega t)) & 0\\
(17.5\cos(\omega t)+10.5)-z & (13.3-14\cos(\omega t)) & -x\\
y & x & -8/3
\end{bmatrix}. \tag{3}
$$

THEOREM 1. *In system (1), the three equilibrium S_0, S_-, S_+ are saddle point in the three-dimensional phase space for all* $\cos(\omega t)\in[-1,1]$.

PROOF.

(i) Linearizing system (1) about the equilibrium S_0 yields an eigenvalue $\lambda_1=-8/3$ along with the following characteristic equation,

$$
\begin{aligned}
f(\lambda)&=\lambda^2+(14\cos(\omega t)-13.3)\,\lambda\\
&\quad-(23.8+3.5\cos(\omega t))\,(25-10\cos(\omega t))\\
&=0.
\end{aligned} \tag{4}
$$

Its other two eigenvalue are

$$\lambda_2 = \frac{1}{2}\Big((13.3 - 14\cos(\omega t)) + \sqrt{(13.3 - 14\cos(\omega t))^2 + 4(23.8 + 3.5\cos(\omega t))(25 - 10\cos(\omega t))}\Big),$$

$$\lambda_3 = \frac{1}{2}\Big((13.3 - 14\cos(\omega t)) - \sqrt{(13.3 - 14\cos(\omega t))^2 + 4(23.8 + 3.5\cos(\omega t))(25 - 10\cos(\omega t))}\Big),$$

respectively, satisfying $\lambda_1 < 0$, $\lambda_2 > 0$, and $\lambda_3 < 0$. So, the equilibrium S_0 is a saddle point in the three-dimensional phase space.

(ii) Linearizing system (1) about the other two equilibria, $S_\pm$, yields the following characteristic equation:

$$\begin{aligned} f(\lambda) &= \lambda^3 + \left(\frac{43.1}{3} + 4\cos(\omega t)\right)\lambda^2 \\ &\quad + \left(\frac{284}{3} + 20\cos(\omega t)\right)\lambda \\ &\quad + \frac{16}{3}(25 - 10\cos(\omega t))(23.8 + 3.5\cos(\omega t)) \\ &= 0. \end{aligned} \tag{5}$$

Thus, the two equilibrium, $S_\pm$, have the same stability property.

Let

$$\begin{aligned} a_0 &= 1, \\ a_1 &= \frac{43.1}{3} + 4\cos(\omega t), \\ a_2 &= \frac{284}{3} + 20\cos(\omega t), \\ a_3 &= \frac{16}{3}(25 - 10\cos(\omega t))(23.8 + 3.5\cos(\omega t)). \end{aligned}$$

We observed that

$$a_0 > 0, \qquad a_1 > 0, \qquad a_3 > 0, \qquad a_4 > 0.$$

While

$$\begin{aligned} a_1 a_2 - a_3 &= \left(\frac{43.1}{3} + 4\cos(\omega t)\right)\left(\frac{284}{3} + 20\cos(\omega t)\right) \\ &\quad - \frac{16}{3}(25 - 10\cos(\omega t))(23.8 + 3.5\cos(\omega t)) \\ &= -320a^2 - 410a - 5440 \\ &< 0. \end{aligned}$$

According to the Routh-Hurwitz conditions, the other two equilibrium $S_\pm$ are both saddle points in the three-dimensional phase space.

THEOREM 2. *In system (1), the Jacobian at $S_{\pm}$ has a real eigenvalue, $\lambda_R < 0$, and a complex-conjugate pair of eigenvalues, $(\lambda_C)_{\pm} = \sigma \pm \psi i$, where $|\lambda_R| > \sigma > 0$.*

PROOF. From (5), let

$$A = \left(\frac{43.1}{3} + 4\cos(\omega t)\right) > 0,$$
$$B = \left(\frac{284}{3} + 20\cos(\omega t)\right) > 0,$$
$$C = \frac{16}{3}(25 - 10\cos(\omega t))(23.8 + 3.5\cos(\omega t)) > 0.$$

Then, we can determine the exact values of the eigenvalues by setting $\lambda = -A/3 + \Lambda$ in (5). This yields

$$f(\lambda) = \Lambda^3 + P\Lambda + Q,$$

where $P = -A^2/3 + B$ and $Q = 2A^3/27 - AB/3 + C$.

This third-order polynomial in Λ can be solved by using the Cardan formula, where one may set

$$\Delta = 4P^3 + 27Q^2.$$

Obviously,

$$\begin{aligned} P &= -\frac{A^2}{3} + B \\ &= \frac{9(284 + 60\cos(\omega t)) - (43.1 + 12\cos(\omega t))^3}{27} \\ &> 0 \end{aligned}$$

and

$$\begin{aligned} Q &= \frac{2A^3}{27} - \frac{AB}{3} + C \\ &= \frac{2}{27}\left(\frac{43.1}{3} + 4\cos(\omega t)\right)^3 - \frac{(43.1/3 + 4\cos(\omega t))(284/3 + 20\cos(\omega t))}{3} \\ &\quad + \frac{16}{3}(25 - 10\cos(\omega t))(23.8 + 3.5\cos(\omega t)) \\ &> 0. \end{aligned}$$

So that

$$\Delta = 4P^3 + 27Q^2 > 0.$$

Consequently, (5) has a unique real eigenvalue,

$$\begin{aligned} \lambda_R &= -\frac{A}{3} + \Lambda_R \\ &= -\frac{A}{3} + \left(-\frac{Q}{2} + \sqrt{\frac{Q^2}{4} + \frac{P^3}{27}}\right)^{1/3} + \left(-\frac{Q}{2} - \sqrt{\frac{Q^2}{4} + \frac{P^3}{27}}\right)^{1/3} \\ &= -\frac{A}{3} + \left(-\frac{Q}{2} + \sqrt{\frac{\Delta}{4 \times 27}}\right)^{1/3} + \left(-\frac{Q}{2} - \sqrt{\frac{\Delta}{4 \times 27}}\right)^{1/3}, \end{aligned} \tag{6}$$

along with two complex complex conjugate eigenvalues,

$$\begin{aligned} (\lambda_C)_{\pm} &= \sigma \pm \psi i \\ &= -\frac{A}{3} + (\Lambda_C)_{\pm} \\ &= -\frac{A}{3} - \frac{\Lambda_R}{2} \pm \frac{i}{2}\sqrt{4P + 3(\Lambda_R)^2}, \end{aligned} \tag{7}$$

where $\sigma = -A/3 - \Lambda_R/2$, $\psi = \pm(1/2)\sqrt{4P + 3(\Lambda_R)^2}$. In (6), $A > 0$, $Q > 0$, and $\Delta > 0$, so

$\lambda_R < 0$, $\sigma = A/3 - \Lambda_R/2 > 0$.

Since $\lambda_R + 2\sigma = -A$, and $\lambda_R < 0$, $\sigma > 0$, we have $|\lambda_R| - 2\sigma = A > 0$. The characteristic eigenvalues of the two equalibria satisfy the Shil'nikov inequalities [11], that is,

$$\lambda_R \sigma < 0 \qquad \text{and} \qquad |\lambda_R| > \sigma > 0.$$

Therefore, the two equalibria are all saddle-foci with an instability index of two, and the negative real eigenvalue is associated with a one-dimensional stable manifold, whereas both complex conjugate eigenvalues, with a two-dimensional unstable manifold in which trajectories are spiraling outwards.

4. IMPULSIVE CONTROL

We shall establish, in this section, some sufficient conditions to stabilize the hyperchaotic system (2) by impulsive control. Let $u = [x\ y\ z]^\top$, and $u(t)$ be a solution of system (2). An impulsive control law of (2) is given by a sequence $\{t_k, B_k u(t_k)\}$, where

$$0 < t_1 < t_2 < \cdots < t_k < t_{k+1} < \cdots, \qquad t_k \to +\infty, \quad \text{as } k \to +\infty$$

and each B_k is a 3×3 constant matrix. It works as follows. Let $u(t) = u(t, t_0, u_0)$ be a solution of system (2) starting at (t_0, u_0). The point $P_t(t, u(t))$ begins its motion from the initial point $P_{t_0}(t_0, u_0)$ and moves along the curve $[(t, u); t \geq t_0, u = u(t)]$ until the time $t_1 > t_0$ at which the point $P_{t_1}(t_1, u(t_1))$ is transferred immediately to $P_{t_1^+}(t_1, u_1^+)$, where $u_1^+ = u(t_1) + B_1 u(t_1)$. Then, the point P_t continues to move further along the curve with $u(t) = u(t, t_1, u_1^+)$ until it triggers a second transfer at $t_2 > t_1$. Once again, the point $P_{t_2}(t_2, u(t_2))$ is mapped into the point $P_{t_2^+}(t_2, u(t_2^+))$, where $u_2^+ = u(t_2) + B_2 u(t_2)$. As before, the point P_t continues to move forward with $u(t) = u(t, t_2, u_2^+)$ as the solution of (2) starting at (t_2, u_2^+). Clearly, this process continues as long as the solution of (2) exists and it results in a piecewise-continuous trajectory $u(t)$, which satisfies the following impulsive system of differential equations,

$$\begin{aligned} \dot{u} &= A(t)\, u + xBu, && t \neq t_k, \\ u\left(t_k^+\right) - u\left(t_k\right) &= B_k u\left(t_k\right), && t = t_k, \end{aligned} \tag{8}$$

where

$$A(t) = \begin{bmatrix} a_{11} & a_{12} & 0 \\ a_{21} & a_{22} & 0 \\ 0 & 0 & a_{33} \end{bmatrix}, \qquad B = \begin{bmatrix} 0 & 0 & 0 \\ 0 & 0 & -1 \\ 0 & 1 & 0 \end{bmatrix},$$

$u(t_k^+) = \lim_{t \to t_k^+} u(t)$, B_k is the impulsive control matrix, $k = 1, 2, \ldots$.

Let $\Delta_k = t_k - t_{k-1}$, and β_k be the largest eigenvalue of $(I + B_k)^\top (I + B_k)$, for all $k = 1, 2, \ldots$. For $t \in [0, +\infty)$, let $\alpha(t)$ be the largest eigenvalue of $A(t)^\top + A(t)$. Since $A(t)$ is periodic, it follows that $\max_{t \in [0, +\infty)} \{\alpha(t)\}$ exits. Let $\alpha_{\max} = \max_{t \in [0, +\infty)} \{\alpha(t)\}$. Then we have the following result.

THEOREM 3. *For the controlled system (8), assume that there exist positive constants l and η, such that for $k = 1, 2, \ldots$,*

$$\Delta_k \leq l$$

and

$$ln\beta_k + \Delta_k (\alpha_{\max} + \eta) \leq 0. \tag{9}$$

Then, the controlled system (8) is globally exponentially stable.

PROOF. Choose the Lyapunov function $V(u) = u^{\top}u$ and let $v(t) = V(u(t))$, $t \in R_+$. Then, for $t \in (t_{k-1}, t_k)$, we have

$$\begin{aligned}
\dot{v}(t) &= (u')^{\top}u + u^{\top}u' \\
&= (A(t)u + xBu(t))^{\top}u \\
&\quad + u^{\top}(A(t)u + xBu) \\
&= u^{\top}A(t)^{\top}u + xu^{\top}B^{\top}u \\
&\quad + u^{\top}A(t)u + xu^{\top}Bu \\
&= u^{\top}\left(A(t)^{\top} + A(t)\right)u \\
&\quad + xu^{\top}\left(B^{\top} + B\right)u \\
&= u^{\top}\left(A(t)^{\top} + A(t)\right)u \\
&\quad + 2x(yz - yz) \\
&= u^{\top}\left(A(t)^{\top} + A(t)\right)u.
\end{aligned}$$

Since $A(t)^{\top} + A(t)$ is a symmetric matrix, we have

$$u^{\top}\left(A(t)^{\top} + A(t)\right)u \leq \alpha(t)u^{\top}u,$$

where $\alpha(t)$ is the the largest eigenvalue of $A(t)^{\top} + A(t)$.

Thus,

$$\begin{aligned}
\dot{v}(t) &\leq \alpha(t)v(t) \\
&\leq \alpha_{\max}v(t), \qquad t \in (t_{k-1}, t_k),
\end{aligned}$$

where $\alpha_{\max} = \max_{t\in[0,+\infty)}\{\alpha(t)\}$.

So,

$$v(t) \leq v\left(t_{k-1}^{+}\right)e^{\alpha_{\max}(t-t_{k-1})}, \qquad t \in (t_{k-1}, t_k). \tag{10}$$

When $t = t_k$, we have

$$\begin{aligned}
v\left(t_k^{+}\right) &= u\left(t_k^{+}\right)^{\top}u\left(t_k^{+}\right) \\
&= \left((I + B_k)u(t_k)\right)^{\top}\left((I + B_k)u(t_k)\right) \\
&= u(t_k)^{\top}(I + B_k)^{\top}(I + B_k)u(t_k).
\end{aligned}$$

Since $(I + B_k)^{\top}(I + B_k)$ is a symmetrical matrix, we have

$$u(t_k)^{\top}(I + B_k)^{\top}(I + B_k)u(t_k) \leq \beta_k u(t_k)^{\top}u(t_k),$$

which implies

$$v\left(t_k^{+}\right) \leq \beta_k v(t_k). \tag{11}$$

By inequalities (11),(13), we get

$$\begin{aligned}
v\left(t_k^{+}\right) &\leq \beta_k v(t_k) \\
&\leq \beta_k e^{\alpha_{\max}(t_k - t_{k-1})}v\left(t_{k-1}^{+}\right) \\
&= \beta_k e^{\alpha_{\max}\Delta_k}v\left(t_{k-1}^{+}\right) \\
&\leq \left(\beta_k e^{\alpha_{\max}\Delta_k}\right)\left(\beta_{k-1}e^{\alpha_{\max}\Delta_{k-1}}\right)v\left(t_{k-2}^{+}\right) \\
&\vdots \\
&\leq \left(\beta_k e^{\alpha_{\max}\Delta_k}\right)\left(\beta_{k-1}e^{\alpha_{\max}\Delta_{k-1}}\right)\cdots\left(\beta_1 e^{\alpha_{\max}\Delta_1}\right)v\left(t_0^{+}\right).
\end{aligned} \tag{12}$$

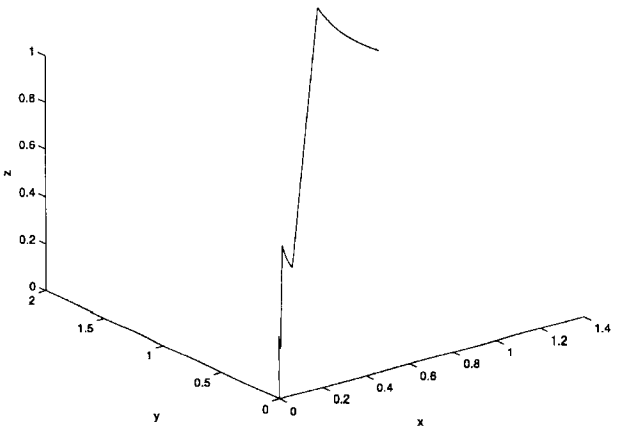

(a) $x - y - z$.

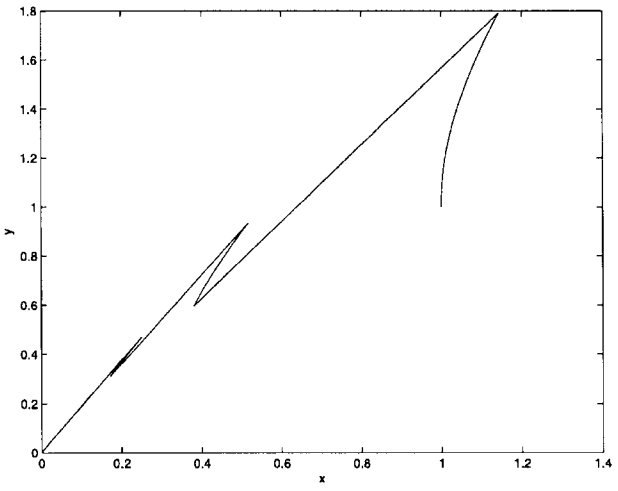

(b) $x - y$.

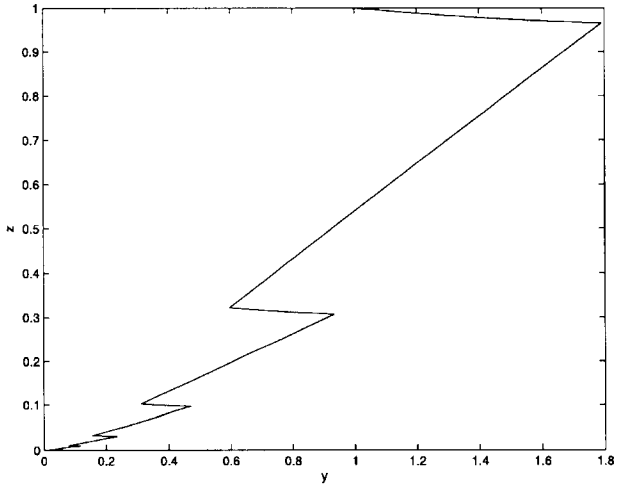

(c) $y - z$.

Figure 6. Phase portraits of controlled system (8).

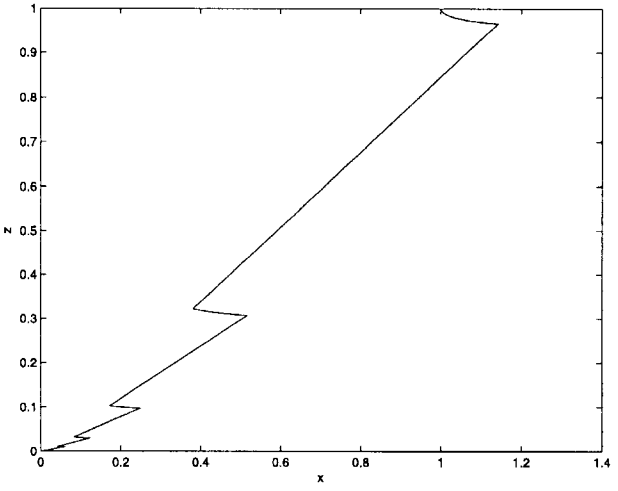

(d) $x - z$.

Figure 6. (cont.)

This, together with condition (9), implies, for $t \in (t_{k-1}, t_k)$,

$$\begin{aligned} v(t) &\leq e^{\alpha_{\max}(t-t_{k-1})} \left(\beta_{k-1} e^{\alpha_{\max}\Delta_{k-1}}\right) \ldots \left(\beta_1 e^{\alpha_{\max}\Delta_1}\right) v\left(t_0^+\right) \\ &\leq e^{(\alpha_{\max}+\eta)(t-t_{k-1})} e^{-\eta(t-t_{k-1})} e^{-\eta\Delta_{k-1}} \ldots e^{-\eta\Delta_1} v\left(t_0^+\right) \\ &\leq e^{(\alpha_{\max}+\eta)l} e^{-\eta(t-t_0)} v\left(t_0^+\right). \end{aligned}$$

Let $M > 0$, such that

$$e^{(\alpha_{\max}+\eta)l} = M^2.$$

Then, we get by (13),

$$\|u(t)\| \leq M e^{-1/2\eta(t-t_0)} \|u_0\|, \qquad t \geq t_0. \tag{14}$$

Therefore, the controlled system (8) is globally exponentially stable.

Next, by impulsive control, some numerical simulations for controlled chaos system (8) are obtained. The system parameters are chose as follows, $W = 1$, the impulsive control matrix $B_k = -2/3I$, and the impulsive time intervals $\Delta_k = 0.03$, for all $k = 1, 2, \ldots$. By computing, we have

$$\alpha_{\max} = 60.6028, \qquad \beta_k = \frac{1}{9}.$$

So for $\eta = 12.64$,

$$ln\beta_k + \Delta_k (\alpha_{\max} + \eta) \leq 0.$$

By Theorem 3, the controlled system is globally exponentially stable. The phase portraits are shown in Figure 6. The state orbits of the system are depicted in Figure 7.

In addition, we choose constant $\eta = 3.51$. By inequality (9), the system is globally exponentially stable, if β_k and Δ_k satisfy that $\beta_k e^{\alpha_{\max}\Delta_k} \leq e^{-\eta}$, as shown in Figure 8.

β_k is relevant with the magnitude of the impulsive. Assume $B_k = -\lambda_k I$ $(\lambda_k > 0)$, where λ_k denote the magnitude of the impulsive. We have

$$\beta_k = (1 - \lambda_k)^2.$$

Then,

$$(1 - \lambda_k)^2 e^{\alpha_{\max}\Delta_k} \leq e^{-\eta}.$$

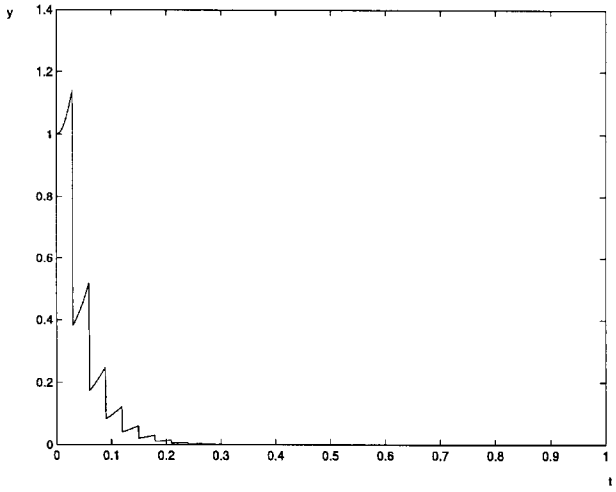

(a) $t - x$.

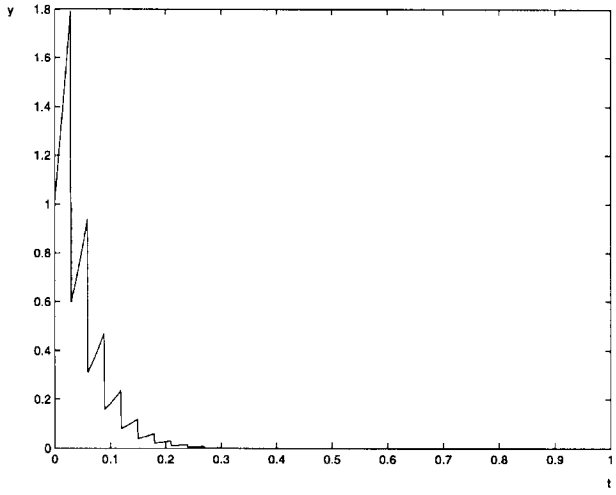

(b) $t - y$.

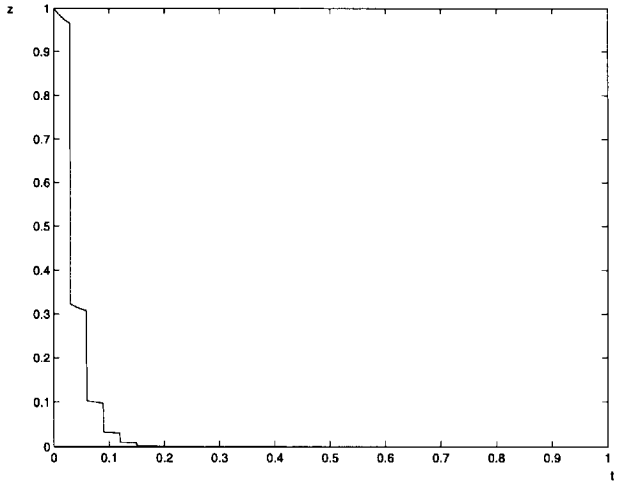

(c) $t - z$.

Figure 7. State orbits of controlled system (8).

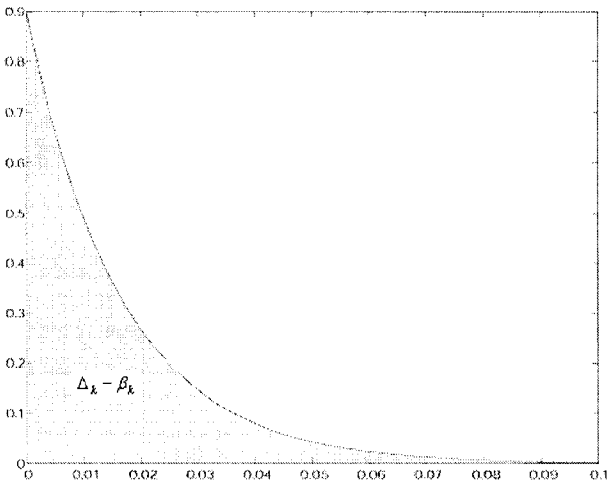

Figure 8. The portrait of β_k and Δ_k.

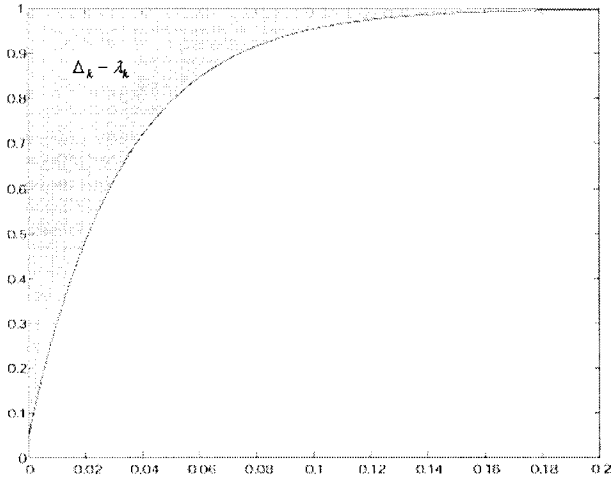

Figure 9. The portrait of β_k and Δ_k.

The portrait of λ_k and Δ_k is shown in Figure 9.

REFERENCES

1. D. Cafagna and G. Grassi, New 3D-scroll attractors in hyperchaotic Chua's circuits forming a ring, *Int. J. Bifurcation and Chaos* **13** (10), 2889–2903, (2003).
2. K. Thamilmaran, M. Lakshmanan and A. Venkatesan, Hyperchaos in a modified canonical Chua's circuit, *Int. J. of Bifurcation and Chaos* **14** (1), 221–243, (2004).
3. O.E. Rossler, An equation for hyperchaos, *Phys. Lett. A* **71** (2-3), 155–157, (1979).
4. C. Barbara and C. Silvano, Hyperchaotic behaviour of two bi-directionally Chua's circuits, *Int. J. Circuit Theory and Applications* **30** (6), 625–637, (2002).
5. A. Khadra, X.Z. Liu and X.M. Shen, Robust impulsive synchronization and application to communication security, *Dynam. Contin. Discrete Impuls. Systems, Ser. B Appl. Algorithms* **10**, 403–416, (2003).
6. V.S. Udaltsov, J.P. Goedgebuer, L. Larger, J.B. Cuenot, P. Levy and W.T. Rhodes, Communicating with hyperchaos: The dynamics of a DNLF emitter and recovery of transmitted information, *Optics and Spectroscopy* **95** (1), 114–118, (2003).
7. E.M. Shahverdiev, R.A. Nuriev, R.H. Hashimov and K.A. Shore, Adaptive time-delay hyperchaos synchronization in laser diodes subject to optical feedback(s), `arXiv:nlin.CD/0404053 v1 29`, (April 2004).
8. A. Cenys, A. Tamaservicius, A. Baziliauskas, R. Krivickas and E. Lindberg, Hyperchaos in coupled Colpitts oscillators, *Chaos, Solutions and Fractals* **17** (2-3), 349–353, (2003).
9. J.-Y. Hsieh, C.-C. Hwang, A.-P. Wang and W.-J. Li, Controlling hyperchaos of the Rossler system, *Int. J. Control* **72** (10), 882–886, (1999).

10. X.Z. Liu and K.L. Teo, Impulsive control of chaotic system, *Int. J. of Bifurcation and Chaos* **12** (5), 1181–1190, (2002).
11. G. Grassi and S. Mascolo, A systematic procedure for synchronizing hyperchaos via observer design, *J. of Circuits, Systems, and Computers* **11** (1), 1–16, (2002).
12. Y.L. Li, X.Z. Liu and X.M. Shen, Chaos synchronization using impulsive driving and application to secure communications, *Dynam. Contin. Discrete Impuls. Systems, Ser. B Appl. Algorithms* **10**, 899–914, (2003).
13. Y. Li, G. Chen and K.S. Tang, Controlling a unified chaotic system to hyperchaotic (to appear).
14. T. Tsubone and T. Saito, Hyperchaos from a 4-D manifold piecewise-linear system, *IEEE Trans. Circuits and Syst.-I* **45** (9), 889–894, (1998).
15. J. Lü, G. Chen, D. Cheng and S. Celikovsky, Bridge the gap between the Lorenz system and the Chen system, *Int. J. of Bifurcation and Chaos* **12** (12), 2917–2928, (2002).
16. C.P. Silva, Shil'nikov's theorem—A tutorial, *IEEE Trans. Circuits and Syst.* **40**, 675–682, (1993).
17. S. Čelikovský and G. Chen, On a generalized Lorenz canonical form of chaotic systems, *Int. J. of Bifurcation and Chaos* **12** (8), 1789–1812, (2002).